VOL. 5, NO. 4, APRIL 2010 ISSN 1819-6608
ARPN Journal of Engineering and Applied Sciences


www.arpnjournals.com

SIMULATION OF PROGRESSIVE FAILURE PREDICTION OF FILAMENT WOUND COMPOSITE TUBES SUBJECTED TO MULTIPLE LOADING WITH MEMBRANE-FLEXION COUPLING EFFECTS

Umar Farooq and Karl Gregory
Built Environment and Engineering Department, University of Bolton, United Kingdom
E-Mail: uf1res@bolton.ac.uk, k.r.gregory@bolton.ac.uk

ABSTRACT

This study deals with the computational modeling of ply by ply failure prediction of filament wound composite tubes under internal burst pressure and external compressive loads with consideration to bending shear. Plates and beams resist transverse load through flexural bending while pressure vessels, pipes, domes, caps and shell like structural composite elements react to the load through membrane forces. Bending stresses are usually neglected in studying behaviour of such elements despite the fact that the bending stresses affect damage modes. Standard failure criteria do not exist for the fibre reinforced composite structural elements hence failure predictions are somewhat unreliable. To consider the flexural shear stresses, methodology of comparative approach involving comparison of failure predictions was adopted. Failure predictions from Tsai-Hill and Tsai-Wu criteria were complemented herein with comparison from Hashin's criteria, which utilize such bending stresses. Interaction of the internal pressure and compressive loads were incorporated into the commercially available finite element analysis software 'ABAQUS^{TM}. To evaluate the effect of loads on deformation and induced changes in tubes, the framework of analysis based on the finite element method provides an exciting capability for analyzing the effects of laminates' lay-up, complicated interaction between the formation of multiple matrix-cracks and de-lamination, orientation and shear effects. Simulation model was developed to use the built-in failure prediction facility of the Hashin criteria. Simple steps were carried out using equations of the other failure criteria to calculate and compare strength parameters for failure predictions. The generated results correlated well and have improved the confidence of accuracy. Simulations can be repeated and extended for similar models subjected to multiple loading. One set of the results consisting of eight un-symmetric plies was selected for presentation herein in the form of legend tables, graphs and contour plots. The study indicates that the approach is useful to predict reliable failure predictions and design improvements for composite wound tubes.

Keywords: wound tubes, low velocity impact, finite element simulation, internal pressure, adaptive meshing.

1. INTRODUCTION

Light-weight, high stiffness and high strength fibrous composites are being widely used in the construction of pressure vessels such as hollow cylindrical tubes for military and civilian applications. A primary use of wound tube is the fabrication of pressure containment structures such as rocket motor cases, launch tubes, and cold storage vessels. The tube casings are used for burning solid propellants, where both design parameters are important. The solid fuel burns and creates high pressure. This causes large hoop strains and expansion in the diameter of the casing. If this expansion is allowed, the propellant would crack due to increased burning rate build up pressure. Casings made from isotropic materials can reduce the expansion by using very thick casings which is not an acceptable solution. However, filament-wound casings made of composite materials can reduce the expansion due to the orthotropic nature of composites without resorting to large thicknesses. The tubes are built with laminates having several layers with various orientations, the layer orientations are chosen to provide adequate stiffness and strength in the direction of the applied loads, taking into account that the composite material is much stronger and stiffer in the fibre direction. The winding angle determines two parameters: resistance to pressure and resistance to expansion in diameter. From the literature review; it was found that improved computational models in the design and analysis of such tubes are direly needed. Some of the relevant studies conducted in this area are given below:

Most of the existing studies of composite cylinders are based on the Lekhnitskii's theory which can be seen in (Lekhnitskii, 1981). Roy and Tsai in (Roy, 1988) proposed a simple and efficient design method for thick composite cylinders for both open-ended (pipes) and closed-ended (pressure vessel) cases. Sayman in (Sayman, 2005) studied the analysis of multi-layered composite cylinders under hygrothermal loading. Xia *et al*., in (Xia, 2001) studied multi-layered filament wound composite pipes under internal pressure. Xia *et al*., in (Xia, 2002) presented an exact solution for multi-layered filament wound composite pipes with resin core under pure bending. Parnas and Katırcı in (Parnas, 2004) discussed the design of fibrous pressure vessels under various loading conditions based on thick-walled, multi-layered, filament wound cylindrical shell.

Roy and Massard in (Roy, 1992) studied the design of thick multi-layered composite spherical pressure vessels based on 3D linear elastic solution using Tsai-Wu failure criterion discovering that hybrid spheres increased the burst pressure. Adali *et al*., in (Adali, 1995) presented another method on the optimization of multi-layered pressure vessels using 3D interactive Tsai-Wu failure

criterion to predict the maximum burst pressure. Sun *et al*., in (Sun, 1999) calculated the stresses and the burst pressure of filament wound solid-rocket motor cases using maximum stress failure criteria and stiffness-degradation model. The effect of surface cracks on strength was investigated theoretically and experimentally for glass/epoxy filament wound pipes, by Tarakçioğlu *et al*., in (Tarakçioğlu, 2000). Mirza *et al*., in (Mirza, 2001) investigated the composite vessels under concentrated moments applied at discrete lug positions using the finite element method. Experimental and computational studies were carried out by Aziz *et al*., in (Aziz, 2008) to predict failure of the composite tubes. Most of the existing studies in the literature are experimental, time consuming, expensive and lack in reliable failure predictions. A simulation model consisting of ply by ply prediction of strength parameters efficiently is needed.

Current study complements the existing research and focuses on developing simulation model considering coupling effects on progressive failure prediction of cylindrical wound tubes to improve predictions for reliable designs.

2. DAMAGE AND PROGRESSIVE FAILURE MODES AND HASHIN'S FAILURE CRITERIA

Damage modes may occur in matrix tensile cracking, matrix compressive/shear failure, ply separation (delamination) and fibre breakage (tensile or compressive). Interalamina (ply) failure can occur by fibre breakage, cracking of matrix, and de-bonding between fibre and matrix. Interlaminer failure occurs by delamination. Fibre breaking occurs for all systems where fibre fracture strain is less than matrix fracture strain. Fibre breakage manifests itself as deviation from linear stress-strain or load-deflection curve. Composites with brittle matrix and high-strain-to-failure fibre fail by matrix cracking of the matrix. Matrix cracking is promoted by the tri-axial stresses generated by constraint fibres. Matrix cracking does not have much effect on load-deformation or stress-strain curve since the strength contribution of the matrix is small compared to the fibre. Fibre breakage and matrix cracking result in total failure. Weak interfaces between fibre and matrix lead to de-bonding. In a longitudinal tensile test of a uni-directional composite no evident de-bonding is apparent in load-deflection curve. Failure surfaces exhibiting fibre pullout is the usual evidence for de-bonding. De-bonding is promoted by different Poisson ratios between fibre and matrix which lead to tensile stresses across the fibre-matrix interface. Under these conditions, all six stress components are generally necessary to characterize and discriminate among the various possible failure modes.

2.1 Fibre failure modes

The fibre tensile mode is assumed to depend only on the axial stress, and the fibre tensile failure is predicted when

$$\left[\frac{\sigma_1}{S_1^l}\right]^2 = 1 \quad (1)$$

Where S_1^l is the axial tensile strength?

This criterion is applicable when σ_1 is positive, and is used to predict a failure mode characterized by fibre breakage. When fibre failure in tension is predicted in a layer, the load carrying capacity of that layer is completely eliminated. The axial modulus E_a, the transverse modulus E_t, the shear modulus G_a and the transverse shear modulus G_t are all reduced to zero. When σ_1 is compressive it is assumed that failure is characterized by fibre buckling and is only depended upon σ_1. The compressive fibre mode failure criterion is governed by the maximum stress criterion

$$\left[\frac{\sigma_1}{S_1^c}\right]^2 = 1 \quad (2)$$

Where S_1^c is the axial compressive strength of the ply. For compressive fibre failure, the layer is assumed to carry a residual axial load, while the transverse load carrying capacity is reduced to zero.

2.2 Matrix failure modes

Matrix failure mode is characterised by cracks running parallel to the fibres. Failure is described as being tensile or compressive, depending upon the sign of the quantity ($\sigma_2 + \sigma_3$). Both matrix mode failure criteria assume quadratic interactions between the thickness, (both in-plane, σ_2 and through the thickness, σ_3), the maximum shear in the transverse plane, and the maximum axial shear. When ($\sigma_2 + \sigma_3$) is positive, the tensile mode criterion is used. This criterion is given by

$$F_t^2 = \left[\frac{\sigma_2+\sigma_3}{S_2^t}\right]^2 + \left[\frac{\tau_{23}^2-\sigma_2\sigma_3}{S_{23}^2}\right] + \left[\frac{\tau_{12}^2+\tau_{31}^2}{S_{12}^2}\right] = 1 \quad (3)$$

Where S_2^t, S_{23} and S_{12} are the transverse tensile, transverse shear and axial strengths, respectively. For ($\sigma_2 + \sigma_3$) negative, the compressive failure criterion is given by

$$F_c^2 = \frac{\left[\frac{\sigma_2-\sigma_3}{2}\right]^2 + \tau_{23}^2}{S_{23}^2} + \left[\frac{\tau_{12}^2+\tau_{31}^2}{S_{12}^2}\right] = 1 \quad (4)$$

This is a simple quadratic interaction between maximum transverse stress and axial shear stress. Failure predicted by the criterion is referred to as compressive/shear failure. No stiffness reduction is assumed after matrix failure occurred. This is because transverse matrix cracks alone usually do not have significant effect on the laminate stiffness.

2.3 Delamination modes

The first possible failure occurs when matrix cracking leads to decrease in the interlaminar strength as a result further loading and deformation causes delamination. Varying the angle between two layers affects the extent of delaminated areas. Maximum delaminated area is observed for laminates with an orientation angle between two adjacent layers being 90^o. Thin laminates showed regular damage pattern with less delaminated area for all types of separation of the bottommost ply from the rest of the laminate. Thicker laminates also shows an increased delaminated area. All the simulated tests show a difference in delaminated area by varying the orientation angle there is no significant effect on the delaminated area. The delamination crack runs in the resin-rich area between plies with different fibre orientation. It has been observed that delamination only occurs in the presence of matrix cracks. Taking this into consideration, the initiation of the delamination mode is determined by scaling the matrix damage functions to higher level of stresses. For $(\sigma_2 + \sigma_3)$ positive, the tensile shear delamination mode is given by

$$S^2 F_t^2 = 1 \tag{5}$$

For $(\sigma_2 + \sigma_3)$ negative, the compressive/shear delamination mode is given by

$$S^2 F_t^2 = 1 \tag{6}$$

Where F_t and F_c are damage functions and S is used as scale factor which can be determined from fitting the analytical prediction for the numerical data for the delamination area. When delamination is predicted, the transverse modulus, the axial and transverse shear moduli are reduced to zero in the layer with matrix damage. However, the layer axial modulus is unchanged. The criteria can be extended to 3D problems.

2.4 Hashin's failure criteria (Hashin, 1980)

The failure modes included in Hashin's criteria are as follows:

Tensile fibre failure for $\sigma_{11} \geq 0$

$$\left(\frac{\sigma_{11}}{X_T}\right)^2 + \frac{\sigma_{12}^2 + \sigma_{13}^2}{S_{12}^2} = \begin{cases} \geq 1 & \text{failure} \\ < 1 & \text{no failure} \end{cases} \tag{7}$$

Compressive fibre failure for $\sigma_{11} < 0$

$$\left(\frac{\sigma_{11}}{X_C}\right)^2 = \begin{cases} \geq 1 & \text{failure} \\ < 1 & \text{no failure} \end{cases}$$

Tensile matrix failure for $\sigma_{22} + \sigma_{33} > 0$

$$\frac{(\sigma_{22} + \sigma_{33})^2}{Y_T^2} + \frac{\sigma_{23}^2 - \sigma_{22}\sigma_{33}}{S_{23}^2} + \frac{\sigma_{12}^2 + \sigma_{13}^2}{S_{12}^2} = \begin{cases} > 1 & \text{failure} \\ \leq 1 & \text{no failure} \end{cases} \tag{8}$$

Compressive matrix failure for $\sigma_{22} + \sigma_{33} < 0$

$$\left[\left(\frac{Y_C}{2S_{23}}\right)^2 - 1\right]\left(\frac{\sigma_{22} + \sigma_{33}}{Y_C}\right) + \frac{(\sigma_{22} + \sigma_{33})^2}{4S_{23}^2} + \frac{\sigma_{23}^2 - \sigma_{22}\sigma_{33}}{S_{23}^2} + \frac{\sigma_{12}^2 + \sigma_{13}^2}{S_{12}^2} = \begin{cases} > 1 & \text{failure} \\ \leq 1 & \text{no failure} \end{cases} \tag{9}$$

Interlaminar tensile failure for $\sigma_{33} > 0$

$$\left(\frac{\sigma_{33}}{Z_T}\right)^2 = \begin{cases} > 1 & \text{failure} \\ \leq 1 & \text{no failure} \end{cases} \tag{10}$$

Interlaminar compression failure for $\sigma_{33} < 0$

$$\left(\frac{\sigma_{33}}{Z_C}\right)^2 = \begin{cases} > 1 & \text{failure} \\ \leq 1 & \text{no failure} \end{cases} \tag{11}$$

Where σ_{ij} denote the stress components and the tensile and compressive allowable strengths for lamina are denoted by subscripts *T* and *C*, respectively. X_T, Y_T, Z_T denotes the allowable tensile strengths in three respective material directions. Similarly, X_C, Y_C, Z_C denotes the allowable tensile strengths in three respective material directions. Further, S_{12}, S_{13} and S_{23} denote allowable shear strengths in the respective principal material directions.

A shortcoming of Tsai-Hill and Tsai-Wu criteria is that they do not explicitly differentiate matrix failure from fibre failure. Hashin's criterion decomposes into separate fibre and matrix failure modes. It also distinguishes tensile states from compressive states, which separate criterion taken for each. This then involves more terms than just those in Tsai-Wu; several assumptions were used to bring the parameter count down to a manageable level of the six properties. Hashin developed a set of interactive failure criteria in which distinct failure modes are modelled and defined a general failure criterion in terms of the stress invariants. The five stress invariants (I_1, I_2, I_3, I_4, and I_5) are:

$$\begin{aligned} I_1 &= \sigma_{11}, \\ I_2 &= \sigma_{22} + \sigma_{33}, \\ I_3 &= \sigma_{22}^2 + \sigma_{33}^2 + 2\sigma_{23}^2, \\ I_4 &= \sigma_{12}^2 + \sigma_{13}^2, \\ I_5 &= \sigma_{22}\sigma_{12}^2 + \sigma_{33}\sigma_{13}^2 + 2\sigma_{12}\sigma_{13}\sigma_{23}. \end{aligned} \tag{12}$$

The I_5 invariant does not appear in the criterion because only linear and quadratic terms are retained in this polynomial. To identify distinct failure modes, Hashin argued that failure is produced by the normal and shear stresses acting on the failure plane. For failure parallel to the ply, the failure plane is the 2-3, acted on by stresses σ_{11}, σ_{12}, and σ_{13}. The perpendicular stresses (σ_{22}, σ_{23}, and σ_{33}) do not contribute to parallel failure.

Reviewing the literature for existing failure theories the set of criteria Hashin was also selected for this study. For delamination prediction Hashin's failure criteria satisfies the requirements for effective use of transverse shear stresses in addition to membrane failures.

3. COMPUTATIONAL PROCEDURE FOR STRESSES AND FAILURE PREDICTIONS

Every material has certain strength, expressed in terms of stress or strain, beyond which it fractures or fails. An object is regarded failed when it can no longer support the loads acting on it or when the component can no longer fulfil the function for which it was designed. Such failures include excessive deflection as seen when a laminate buckles, or even just matrix cracking. The latter could constitute failure for a container because any contents would be able to leak through the matrix cracks in the container's walls. Failure theories for isotropic materials are independent of the direction and are characterized by yield strength. A large number of such criteria exist but no one criterion being universally satisfactory for composites.

Failure predictions of composites start by considering a single ply before moving on to laminates. The laminate to be a regular array of parallel continuous fibres perfectly bonded to the matrix have five basic modes of failure of such a ply: longitudinal tensile or compressive, transverse tensile or compressive, or shear. Each of these modes would involve detailed failure mechanisms associated with fibre, matrix or interface failure. First step is to calculate the stresses/strains in the material principal directions. This can be done by transformation of stresses from the global coordinates to local material coordinates of the ply. The constitutive equations are used to calculate the stresses in each ply when the values of the loads acting on the laminate are known. A flowchart for the procedure of stresses and strains in individual ply owing to external loads used to streamline calculations is shown below:

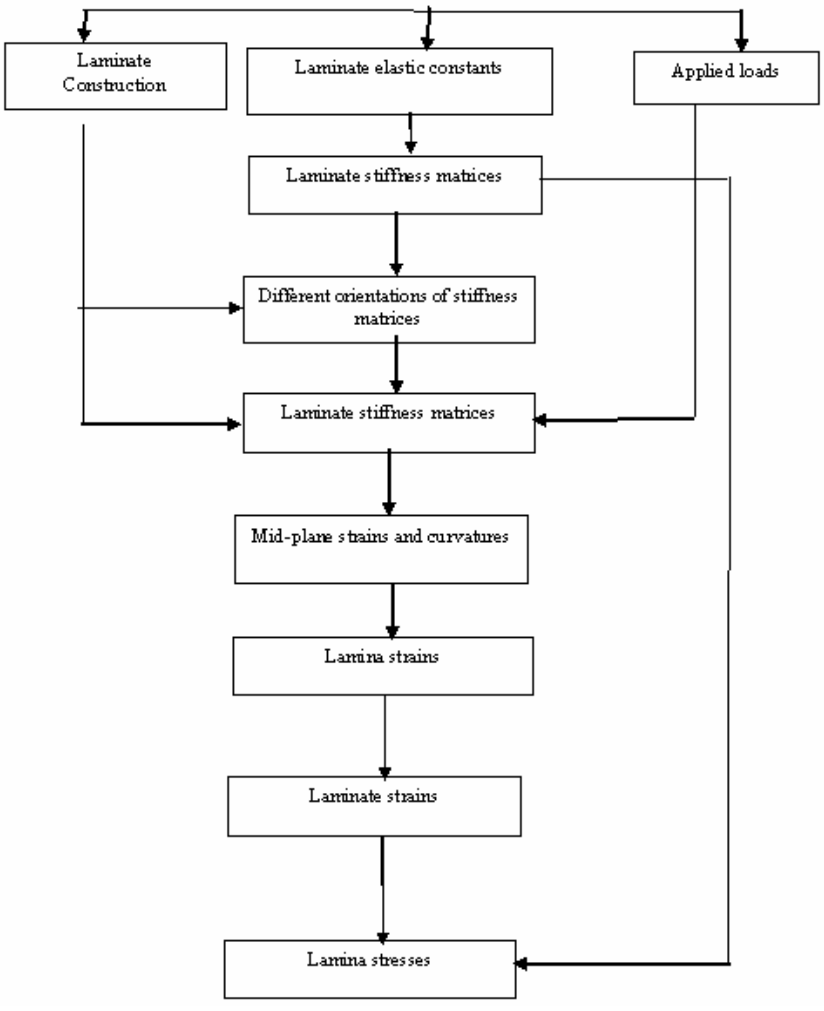

Flowchart-1. Flowchart for laminate stress analysis (Agarwal, 2006).

These stresses and strains can be used to predict the load at which failure initiates, first lamina fails, compared with the corresponding allowable values.

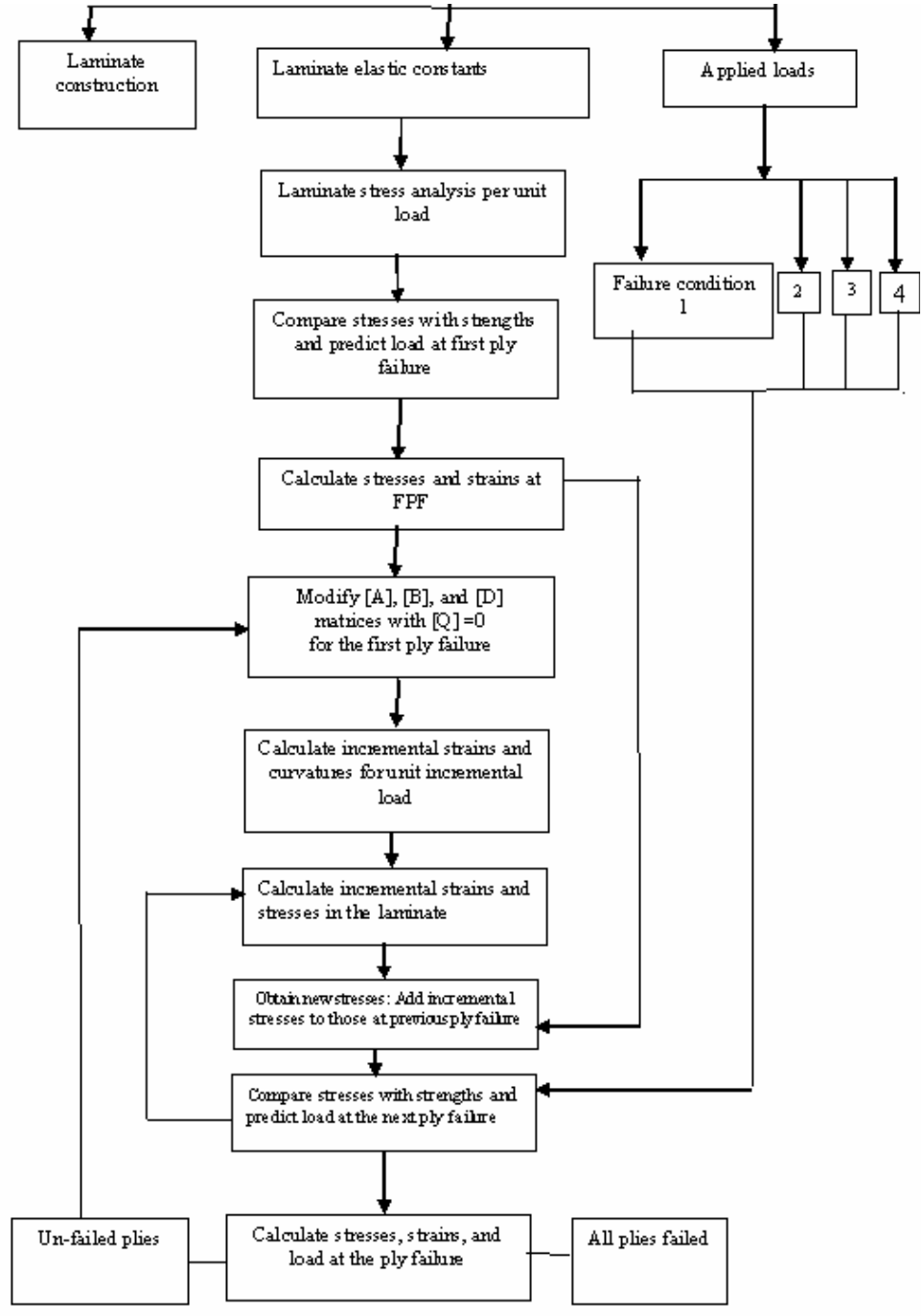

Flowchart-2. Flowchart for laminate strength analysis (Agarwal, 2006).

The determination of the ultimate failure of laminate requires an iterative procedure taking into account the damage progression in the various plies. The computational procedure for the multiple ply failure approach for the case of a symmetric laminate under in-plane loading is illustrated by the flowchart and consists of the following steps:

- The load required to produce first ply failure is determined from the lamina stresses using a selected failure criterion. The lamina stresses are obtained as a function of the loading and are referred first to the laminate coordinates and then transformed to the lamina coordinates;
- The failed lamina or laminas are replaced with laminas of reduced stiffness. These usually are the matrix-dominated stiffness, the stiffness reduction factors can be selected based on analysis as completely (ply

discount method). New laminate stiffness matrices are then calculated;

- Lamina stresses are recalculated and checked against the selected failure criterion to verify that the undamaged laminas do not fail immediately under their increased share of stress following the first ply failure;
- The load is increased until the next ply failure occurs and steps 1, 2, and 3 above are repeated; and
- When the remaining undamaged laminas, at any stage of the progressive ply failures, cannot sustain the stresses, ultimate failure of the laminate occurs.

Multidirectional laminate is initiated in the layer (or layers) with the highest stress normal to the fibres. Failure initiation takes the form of distributed micro-cracks with coalesce into micro cracks in the case of a unidirectional lamina under transverse tension while macrocracking extends across the thickness of the layer constitutes.

5. RESULTS AND DISCUSSIONS

Simulation selected for presentation are from a small size specimen tube of 1000 mm long, 200 mm radius, and 2 mm thick consisting of eight non-symmetric ply as shown in Figure-1. Specimen properties assigned to the model are of fabric code "IM7/8552" given in Table-1. Configuration of 8-ply non-symmetric lay-up [45/0/-45/90/45/0/-45/90] with 0.2% strain allowance chosen for discussion herein. The chosen lay-up provides different laminate stiffness for in the other configurations, but de-lamination remains confined to the [0^0/90^0] interfaces. The tube was fixed at the one end and subjected to a range of compressive loads from 100 kN up to 500 kN along with a constant internal pressure of 2 MPa as shown in Figure-4.

Table-1. Material properties used in the analysis.

Property		IM7/8552
Tensile modulus (E_1)	GPa	150
Tensile modulus (E_2)	Gpa	15
Tensile modulus (E_3)	Gpa	15
In-plane shear modulus (G_{12})	Gpa	5.70
In-plane shear modulus (G_{13})	Gpa	5.70
In-plane shear modulus (G_{23})	Gpa	7.26
Poisons ratio (ν_{12})		0.33
Poisons ratio (ν_{13})		0.033
Poisons ratio (ν_{23})		0.033
Ultimate tensile strength	GPa	1500
Ultimate compressive strength	GPa	1500
Ultimate tensile lateral strength	GPa	40
Ultimate compressive lateral strength	GPa	246
Ultimate shear strength	GPa	68

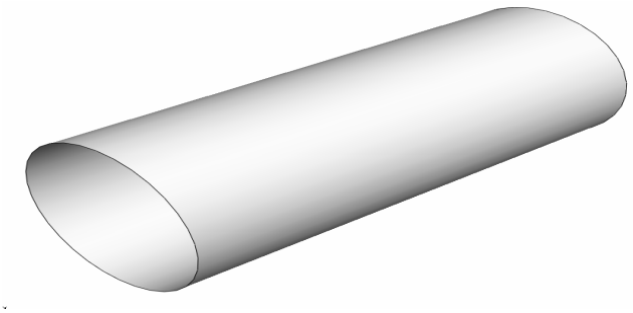

Figure-1. Tube consisting of 8 plies.

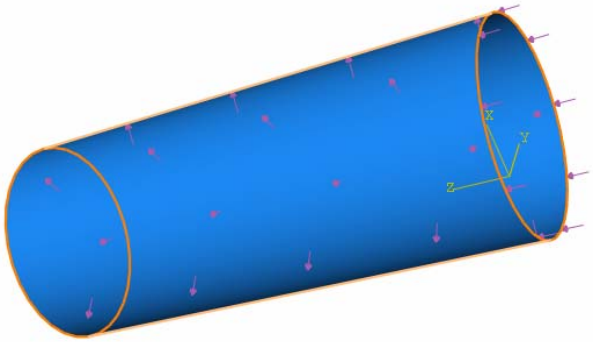

Figure-2. Tube under internal and external compressive loads.

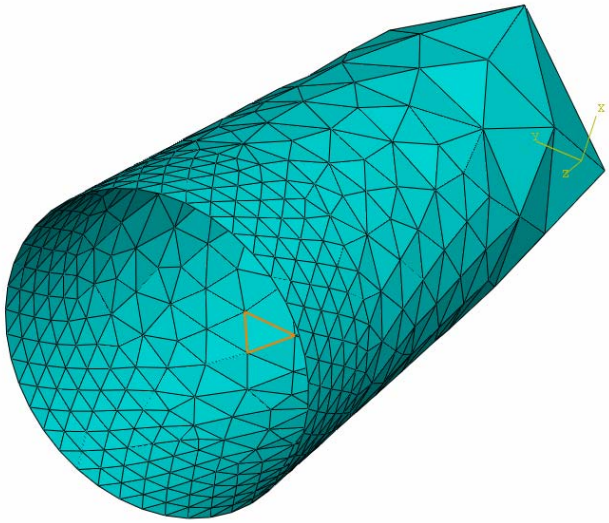

Figure-3. Meshed tube consisting of S_4 shell elements with fine meshes.

The tube was meshed with course elements first but automatic adaptive meshing facility was utilized to finely mesh the tube where load intensity is higher.

First, simulations were carried out in ABAQUS ™ to compute stresses and strains without using built-in Hashin failure criteria. Simulations were performed with incremental load addition until complete failure was reached. Then, simulations were repeated with Hashin's failure criteria. Comparison of ply-by-ply legend

Tables and simulated contour plots from Maximum Strain theory for allowable strains and Hashin's failure theory for strength ratios are shown in Figures 3, 11 below. Failure for all the plies was demonstrated by the simulation as expected under the coupled loads. Simulations were also performed to observe variation of strain energy as shown in Graph 1 and total energy shown in Graph-2. The graphical variation of strain and total energy are acceptable and according to the expectations which validated the models.

Computer generated in-plane normal and shear stresses were used to calculate strength ratios from the standard Tsai-Hill and Tsai-Wu criteria as shown in Table-2. Finally, computed and simulated values for failure theories were compared in Graph-3. The graph demonstrates that Tsai-Hill and Tsai-Wu predicts the similar failure pattern from ply 1 to ply 8 as bending stresses are ignored in these criteria. However, graph line for Hashin's criteria depicts a significant difference in ply 7 and 8. As Hashin criteria regards bending stress acting on the these bottom plies. This further confirms that the bending stresses could cause premature failure and should not be neglected.

The results show that strength parameters correlate changes of material properties according to loading variations. Calculated values were compared against the given strength parameters and failure were found as expected.

Simulated legend Tables and contour plots for comparison of Max strain and hashin failure criteria

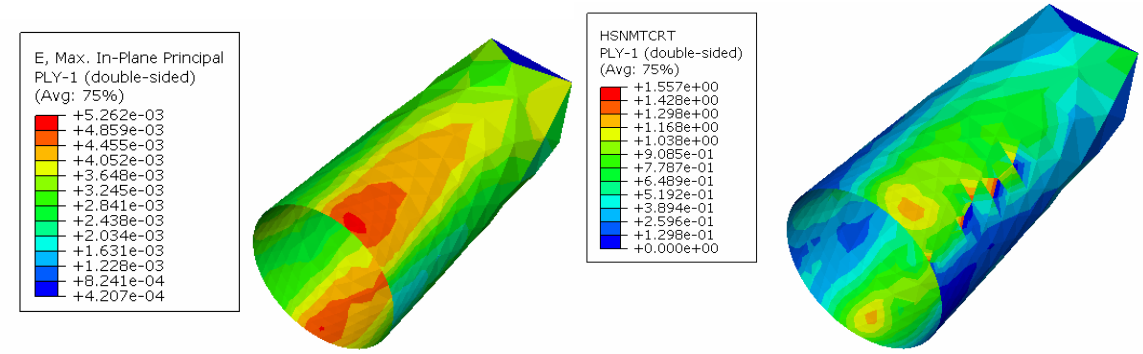

Figure-4. Comparison of legend table and contour plots for ply 1.

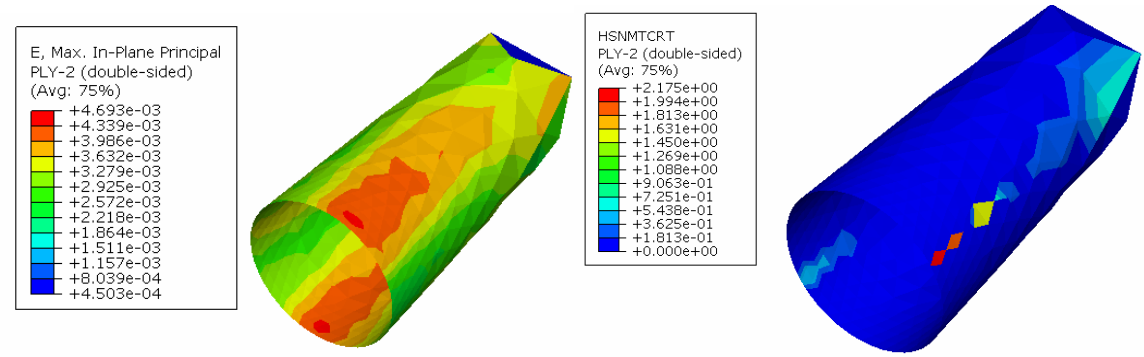

Figure-5. Comparison of legend table and contour plots for ply 2.

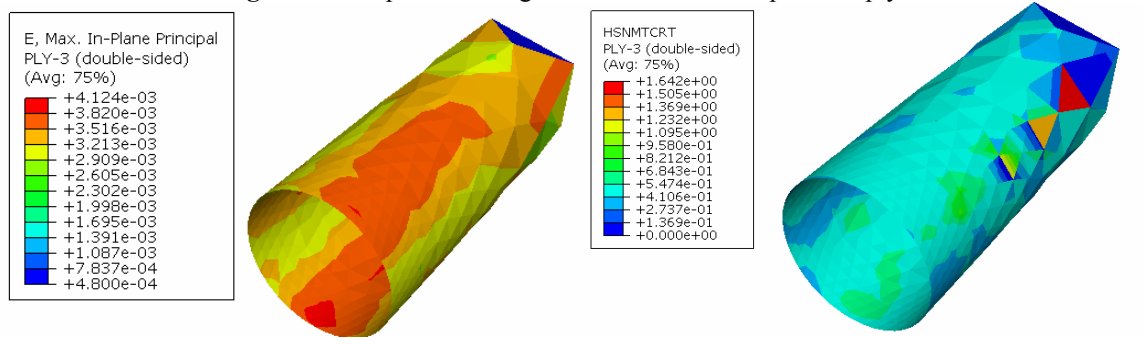

Figure-6. Comparison of legend table and contour plots for ply 3.

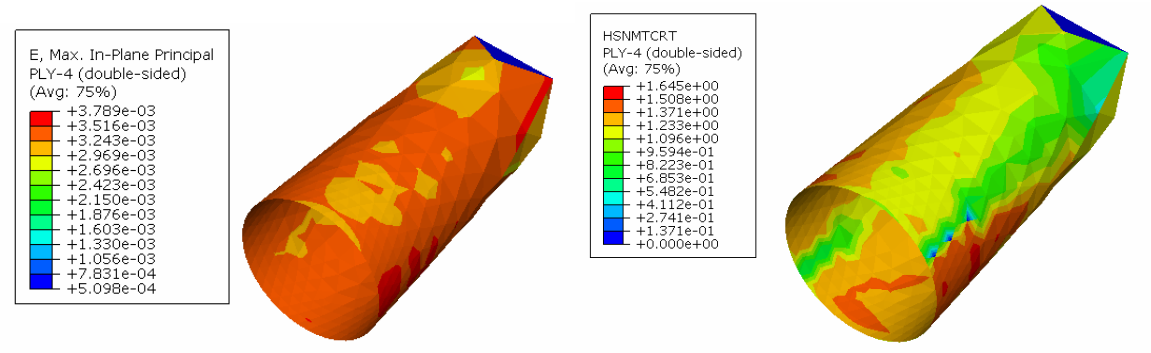

Figure-7. Comparison of legend table and contour plots for ply 4.

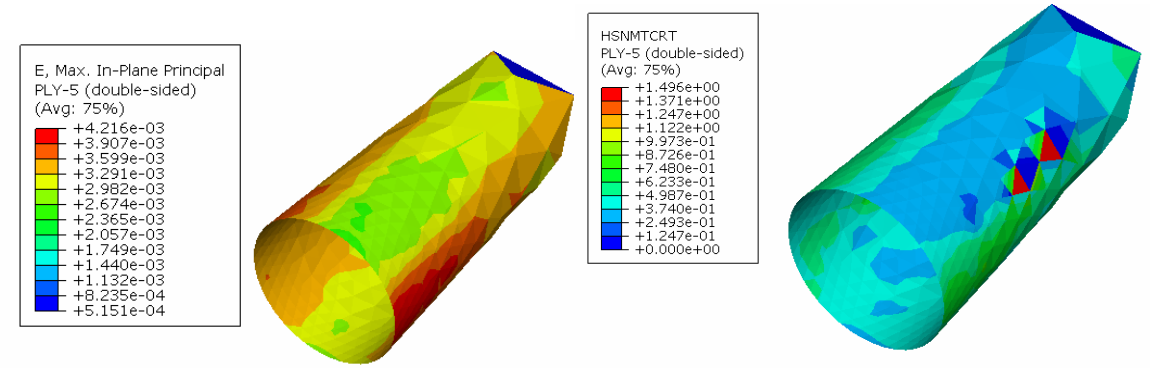

Figure-8. Comparison of legend table and contour plots for ply 5.

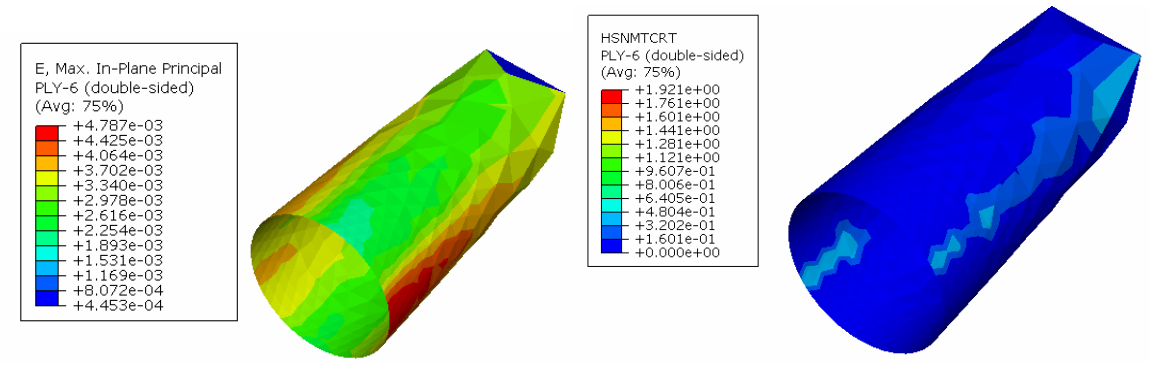

Figure-9. Comparison of legend table and contour plots for ply 6.

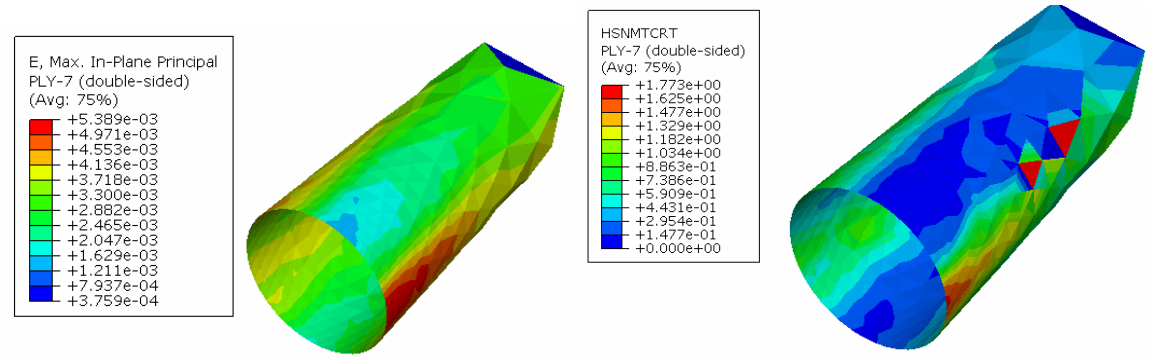

Figure-10. Comparison of legend table and contour plots for ply 7.

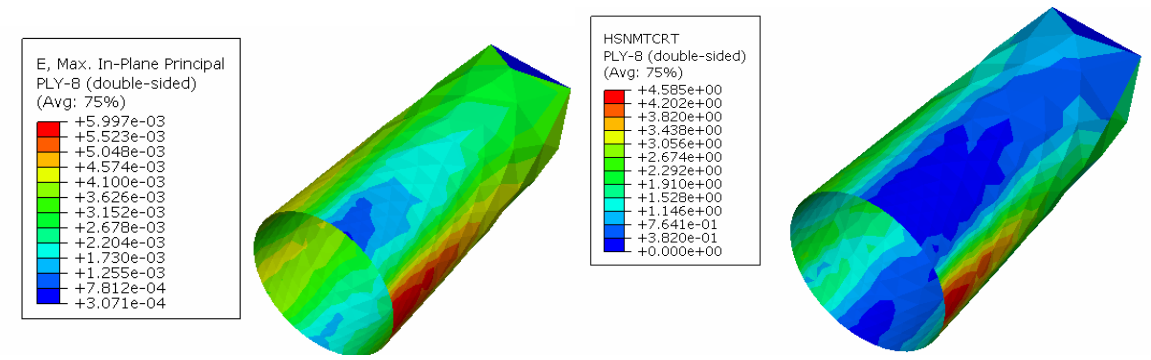

Figure-11. Comparison of legend table and contour plots for ply 8.

Time variation of strain and total energies is shown in the form graphs

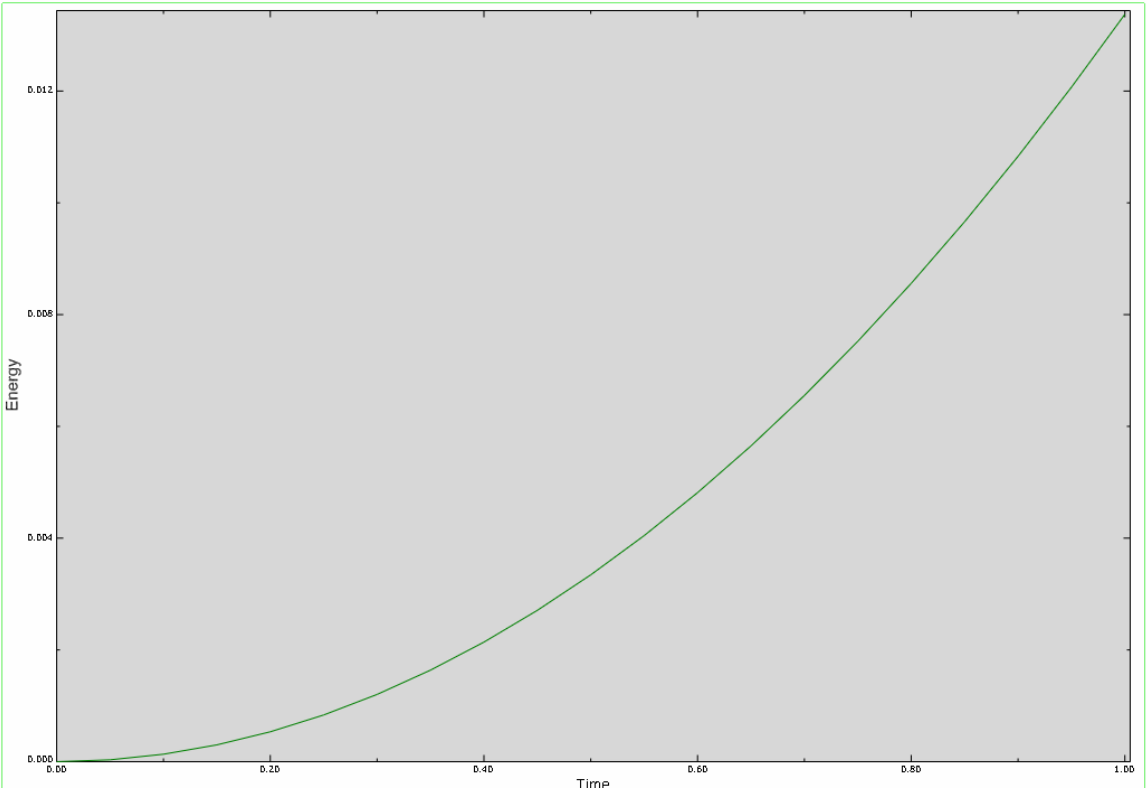

Graph-1. Strain energy (kJ) absorbed by the specimen under load.

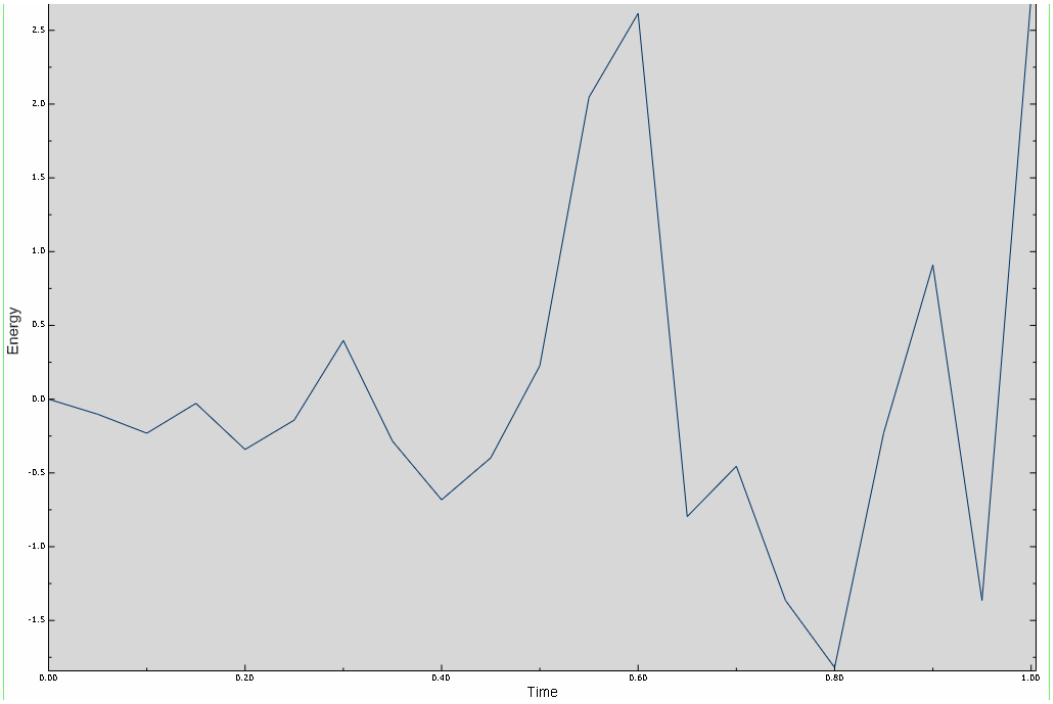

Graph-2. Total energy (kJ) wavy variation under static load.

Table-2. Computed in-plane stresses and strength ratios.

Calculation of strength ratio of Tsai-Wu and Tai-Hill criteria (Agarwall, 2006)					
Ply No.	**σ_{11}**	**σ_{22}**	**σ_{12}**	**Strength ratios**	
	MPa			**Tsai-Wu**	**Tsai-Hill**
1	618	47.3	33.4	1.37	1.81
2	702	59	28.9	1.79	2.57
3	485	50.8	30.6	1.11	1.92
4	555	51.2	24.	1.47	1.90
5	552	48.4	28.4	1.39	1.77
6	717	55.4	29.2	1.7	2.33
7	544	52.5	37.0	1.51	2.15
8	644	85.6	27.3	2.72	2.92

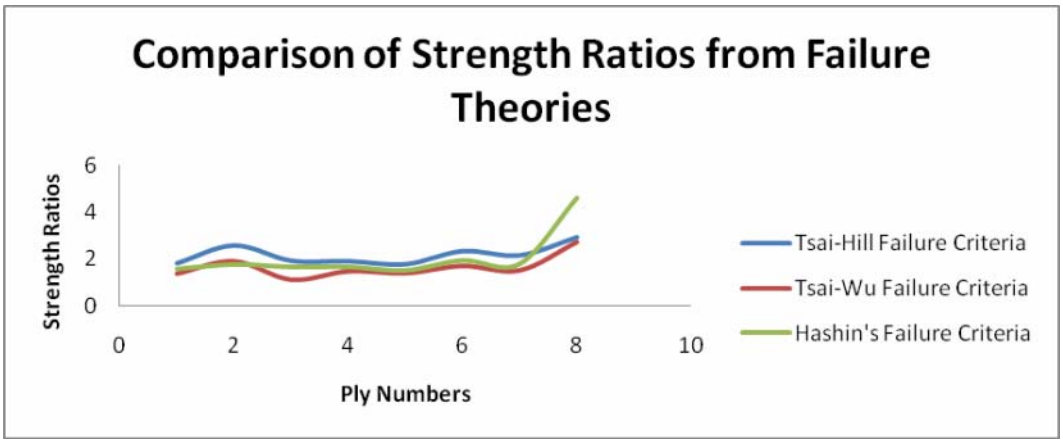

Graph-3. Comparison of strength ratios of the failure criteria.

5. CONCLUSIONS

In this study progressive failure analysis simulation model was developed for a general laminated tube utilising shear stresses. Results for a special case from 8-ply model were illustrated in legend tables, contour plots, tabular and graphical forms. Comparison of standard failure theories was made to predict reliable failures. Results show that for a relatively small range of bottom plies strength ratios for Hashin's criteria are considerably high. This confirms that bending shear has significant effect on failure prediction and could cause failure well below the prediction from the other criteria which neglect the coupling effects.

The analysis methodology has been carried out by assuming that the laminate is composed of identical plies. The analysis can be modified easily if the laminate differs in properties and thickness. Simulations include validation of elastic solution from strain and total energies to analyze the burst pressure when standard values are not available for comparison. The burst pressure varies at higher loads when strength has already decreased. Based on the results it may be further concluded that the tested case is unsafe under these loading conditions.

REFERENCES

Hashin Z. 1980. Failure Criteria for Unidirectional Fibre Composites. ASME Journal of Applied Mechanics. 47(2): 329-334.

S.G. Lekhnitskii. 1981. Theory of elasticity of an anisotropic body, Mir Publishers, Moscow.

A.K. Roy and S.W. Tsai. 1988. Design of thick composite cylinders. J Press Vessel Technol. 110: 255-262. View Record in Scopus | Cited By in Scopus (8).

A.K. Roy and T.N. Massard. 1992. A design study of multilayered composite spherical pressure vessels. J Reinf Plast Compos. 7: 479-493.

S. Adali and V.E. Verijenko *et al*., 1995. Optimization of multilayered composite pressure vessels using exact solution. Compos Press Vessels Ind PVP-V302. pp. 203-312 ASME.

Herakovich C T. 1998. Mechanics of Fibrous Composites. John Wiley and Sons, New York.

X.K. Sun, S.Y. Du and G.D. Wang. 1999. Bursting problem of filament wound composite pressure vessels. Int. J Press Vessels Piping. 76: 55-59.

S. Mirza. 2001. A. Bryan and M. Noori, Fibre-reinforced composite cylindrical vessel with lugs. Compos Struct. 53: 143-151.

M. Xia, H. Takayanagi and K. Kemmochi. 2001. Analysis of multi-layered filament-wound composite pipes under internal pressure. Compos Struct. 53: 483-491.

L. Parnas and N. Katırcı. 2002. Design of fibre-reinforced composite pressure vessels under various loading conditions. Comp Struct. 58: 83-95.

M. Xia, H. Takayanagi and K. Kemmochi. 2002. Bending behavior of filament-wound fibre reinforced sandwich pipes. Comp Struct. 56: 201-210.

O. Sayman. 2005. Analysis of multi-layered composite cylinders under hygrothermal loading. Composites Part A. 36: 923-933.

T.K. Hwang, C.S. Hong and C.G. Kim. 2003. Size effect on the fibre strength of composite pressure vessels. Compos Struct. 59: 489-498.

H. Hahn and S. W. Tsai. 1973. Nonlinear elastic behavior of unidirectional composite laminate. J. Compos. Mater. 7: 102-110.

2004. ABAQUS/Standard User's Manual, Version 6.5, ABAQUS, Inc., Providence, RI.

D. Agarwal Bhagwan, Lawrance J. Brouton and K. Chandrashekkara. 2006. Analysis and Performance of Fibre Composites. 3rd Ed. John-Wiley and Sons, Inc. Hoboken, New Jersy, USA.

Aziz Onder, Onur Sayman, Tolga Dogan and Necmettin Tarakcioglu. 2008. Burst failure of composite pressure vessels. Comp. Struct. 49: 207-228.